Acta Crystallographica Section B
Structural Science
ISSN 0108-7681

Extremely long period-stacking structure in the Sb–Te binary system

Kouichi Kifune,[a]* Yoshiki Kubota,[a] Toshiyuki Matsunaga[b] and Noboru Yamada[c]

[a]Department of Environmental Sciences, Osaka Women's University, Japan, [b]Characterization Technology Group, Matsushita Technoresearch Inc., Japan, and [c]Storage Media Systems Development Center, Matsushita Electric Industrial Co. Ltd, Japan

Correspondence e-mail: kifune@center.osaka-wu.ac.jp

Received 23 March 2005
Accepted 6 June 2005

The crystal structure of the δ-phase in the Sb–Te binary system has been determined by synchrotron powder diffraction. It is clearly shown that many intermetallic compounds, which have different stacking periods depending on compound composition, exist in this phase. These structures are based on the cubic *ABC* stacking structure, and two kinds of fundamental structural units form an intergrowth along the stacking direction at the atomic level. The chemical formulae of these compounds are expressed as $Sb_{2n}Te_3$, where n is an integer and the number of stacking layers is $2n + 3$. There is a relationship of inverse proportionality between the stacking period and the Te concentration.

1. Introduction

Recently, rewritable DVDs (digital versatile disks) have been spreading widely as a new optical recording medium. The recording method has applied a reversible phase change of a material; the phase change between a crystalline phase and an amorphous phase is achieved by temperature control using laser-beam irradiation (Yamada *et al.*, 1991). Sb–Te binary compounds are used as one of the materials for DVDs and are put to practical use by adding Ge, Ag, In *etc*. (Iwasaki *et al.*, 1992; Matsunaga *et al.*, 2001). For compounds to be useful as recording materials, a high-speed phase change at high temperature and the stability of each phase at room temperature are required. These are conflicting requirements; an amorphous phase should crystallize on a nanosecond timescale at high temperature, but on the other hand should keep its state at room temperature for 10 years or more (Matsunaga *et al.*, 2001). Searches for materials having such characteristics have been focused on chalcogenide compounds in view of the similarity of their structures in the crystalline and amorphous phases.

As optical recording materials, $GeTe$–Sb_2Te_3 pseudo-binary compounds and Sb–Te binary compounds with a small amount of Ag, In and Ge are widely used today. These crystalline lattices have a spatially high symmetry and isotropy, a random arrangement of constituent atoms. In addition, lattice vibrations are extremely large in the high-temperature region, which enables these materials to transform from the amorphous to the crystalline phase quickly. On the other hand, amorphous-phase stability is maintained by a complicated covalent bonding network consisting of three or more different kinds of elements; this network has spatial anisotropy and a strong bonding state (Matsunaga & Yamada, 2004). Khulbe *et al.* (2002) have shown that Ge doping of an Sb–Te binary compound improves both properties; the compound that results when around 10% Ge is added to the

eutectic $Sb_{70}Te_{30}$+Sb, which is used as an optical phase-change material, exhibits low jitter and very high amorphous phase stability, retaining a high crystallization speed. However, Sb–Te binary compounds without such small amounts of additives such as Ag, In and Ge lack the above two properties. In the conventional phase diagram of the Sb–Te binary system, it has been reported that the intermetallic compound Sb_2Te_3 exists at 60 at.%Te and the δ phase exists in a wide composition range at around 25 at.%Te (ASM International, 1996). Analysis has shown the structure of Sb_2Te_3 to be the Bi_2Te_3-type structure (Wyckoff, 1963). As concerns the structure of the δ phase, the Sb_2Te compound has been analyzed by the single crystal method (Agafonov *et al.*, 1991), however, on the Sb-rich side, only a high-resolution electron microscopic study has been reported (Nakata *et al.*, 2004), but the precise crystal structure, *i.e.* what the δ phase is, has not yet been determined because the difference between the atomic numbers of Sb and Te is only one; the difference in atomic scattering factors is too small to define the specific lattice site for each atom. Therefore, we have studied several Sb–Te binary specimens in the composition range from 0 to 60 at.%Te, using the anomalous dispersion effect to the maximum extent, in order to clarify the difference in crystal structures between the pure binary compounds and those containing Ag, In and Ge.

2. Experimental

Thin film specimens were formed on glass substrates by the DC sputtering method using Sb–Te alloy targets in an Ar gas atmosphere. By adjusting the composition of the Sb–Te alloy target, eight kinds of specimens with different compositions were prepared. These film specimens were crystallized by laser irradiation and were then scraped off the disk surface with a spatula. Each powdered specimen was packed and sealed into a quartz capillary tube. The other part of the powdered specimen was observed with a transmission electron microscope (Jeol JEM-100C). X-ray diffraction experiments were carried out using a large-diameter Debye–Scherrer camera with an imaging plate at the SPring-8 BL02B2 beamline (Takata *et al.*, 2002). The powdered specimens were heated to 773 K and annealed for 5 min by blowing high-temperature N_2 gas. Measurements were carried out with an incident X-ray wavelength of 0.42137 Å at 300 and 90 K. In the present study, to determine the ordering structure of Sb and Te atoms, the wavelength selectivity that is one of the advantageous features of synchrotron radiation was utilized. Another measurement was carried out for each specimen at the wavelength of 0.40650 Å near the Sb *K*-absorption edge to emphasize the difference of the atomic scattering factor between Sb and Te atoms.

3. Results and discussion

Fig. 1 shows electron diffraction patterns of the $Sb_{72}Te_{28}$ specimen. A single-crystal grain was rotated around the c^* axis, and the patterns from several different directions were obtained. From the analysis of these diffraction patterns, it became clear that this crystal has trigonal symmetry and that all strong spots belong to an *A*7-type structure of Sb (Clark, 1955). A pair of split spots that show the long period structure along the *c* axis was found. As shown in Fig. 1(*b*), since *OP* corresponds to the mean spacing of one atomic layer of the *A*7-type structure and *AB* corresponds to the length of the superlattice, the stacking period of this crystal is about 11 layers (*OP*/*AB* = 10.8; this value is denoted *M* hereafter). Probably, this non-integer *M* value is the result of mixing of some phases with different periods by the fluctuation of the composition.

In Fig. 2, X-ray powder diffraction patterns of all specimens are arranged in order of composition. Each diffraction pattern is similar to that of the Sb specimen, and this result shows that all of these structures resemble the *A*7-type structure of Sb. For the diffraction peaks with weak intensity, it was found that their positions shift with composition. The symbols *O*, *A*, *B* and *P* are attached to the diffraction peaks, as for the case of electron diffraction patterns. *P* is a diffraction peak corre-

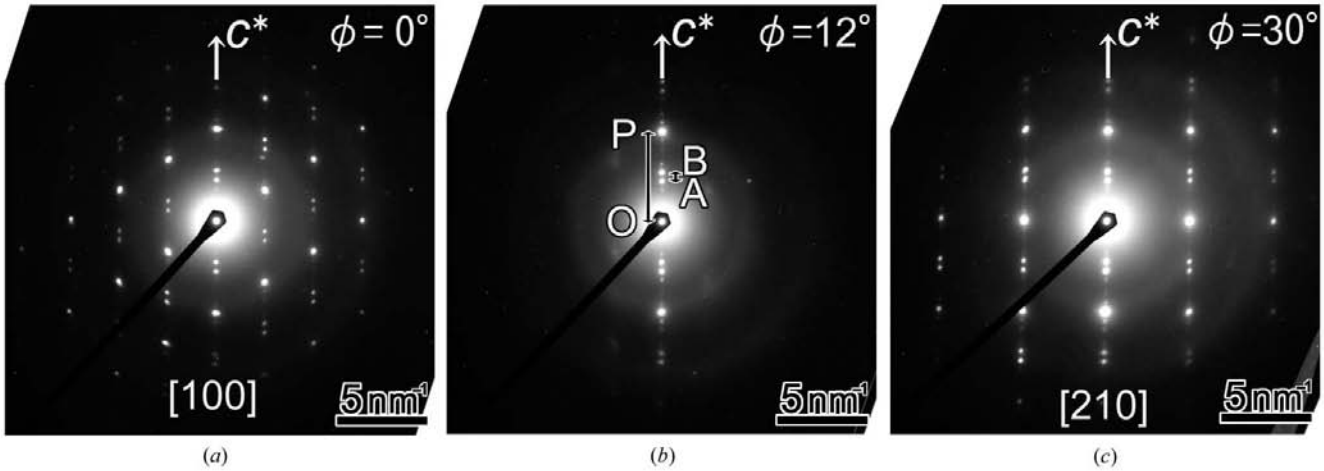

Figure 1
Electron diffraction patterns from a single-crystal grain of $Sb_{72}Te_{28}$. The grain was rotated around the c^* axis, and ϕ indicates the angle of rotation from the [100] direction (*a*). Symbol *P* indicates a fundamental spot, *A* and *B* correspond to superlattice spots.

Table 1
Refined structural parameters for $Sb_{72}Te_{28}$ (11*R*) at 90 K.

The space group is $R\bar{3}m$. Lattice parameters (hexagonal axes) are a = 4.27125 (2) and c = 63.8957 (6) Å. Isotropic displacement parameters of each element are refined as B_{Sb} = 0.67 (1) and B_{Te} = 0.32 (1) Å^2. Reliability factors are R_{wp} = 0.0656 and R_I = 0.0424.

Atom	Site	x	y	z
Te1	3(*a*)	0	0	0
Sb1	6(*c*)	1/3	2/3	0.03290 (4)
Te2	6(*c*)	2/3	1/3	0.05840 (3)
Sb2	6(*c*)	0	0	0.09430 (4)
Sb3	6(*c*)	1/3	2/3	0.11846 (4)
Sb4	6(*c*)	2/3	1/3	0.15457 (4)

sponding to the spacing of a fundamental lattice plane perpendicular to the *c* axis. *A* and *B* are the diffraction peaks reflecting the long period structure along the *c* axis. The distances between the diffraction peaks *A* and *B*, which are indicated by arrows in the figure, become smaller with increasing Sb concentration, and *A* and *B* are merged on the

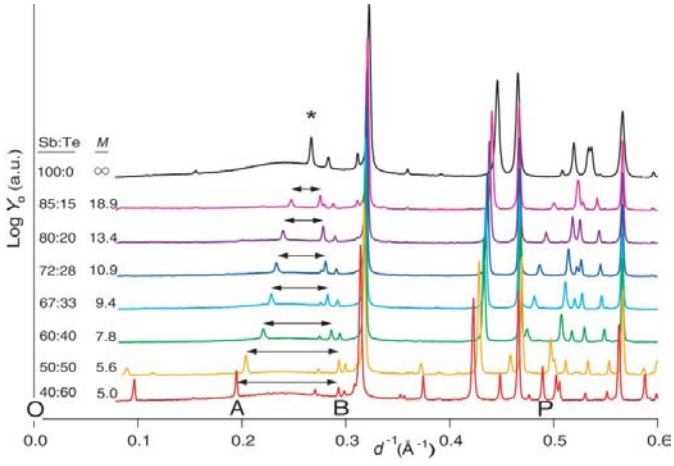

Figure 2
X-ray powder diffraction profile of each specimen at 300 K. The vertical axis is plotted in logarithmic scale to emphasize the weak peaks and each profile is offset in the direction of this axis. The composition and stacking period *M* of each specimen are represented.

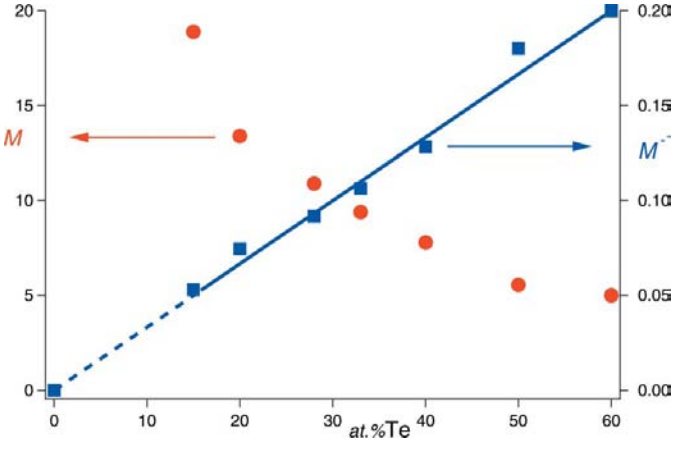

Figure 3
The dependences of stacking period *M* (red solid circle) and M^{-1} (blue solid square) on the Te concentration.

Table 2
Refined structural parameters for $Sb_{85}Te_{15}$ (19*R*) at 90 K.

The space group is $R\bar{3}m$. Lattice parameters (hexagonal axes) are a = 4.28168 (2) and c = 108.7017 (8) Å. Isotropic displacement parameters of each element are refined as B_{Sb} = 0.406 (7) and B_{Te} = 0.20 (2) Å^2. Reliability factors are R_{wp} = 0.0645 and R_I = 0.0334.

Atom	Site	x	y	z
Te1	3(*a*)	0	0	0
Sb1	6(*c*)	2/3	1/3	0.01902 (3)
Te2	6(*c*)	1/3	2/3	0.03413 (3)
Sb2	6(*c*)	0	0	0.05560 (3)
Sb3	6(*c*)	2/3	1/3	0.06931 (3)
Sb4	6(*c*)	1/3	2/3	0.08982 (3)
Sb5	6(*c*)	0	0	0.10426 (3)
Sb6	6(*c*)	2/3	1/3	0.12508 (3)
Sb7	6(*c*)	1/3	2/3	0.13886 (3)
Sb8	6(*c*)	0	0	0.15972 (3)

Sb 003 reflection (this peak is marked by an asterisk on the profile of the Sb specimen). For each specimen, the stacking period *M* (= *OP*/*AB*) calculated from these diffraction peak positions is represented in the figure. The relationship between the composition and *M* value is shown in Fig. 3. The *M* value increases rapidly as the Te concentration decreases.

In Fig. 3, M^{-1} (*i.e.* the reciprocal of *M*) is mostly distributed on the straight line that connects the origin and the point (60, 0.2), which corresponds to Sb_2Te_3 with the 5*R* structure. Thus, M^{-1} and the Te concentration are proportional. When the Te concentration is indicated as C_{Te}(at.%), the following formula is obtained from the slope of this line

$$1/M = (C_{Te}/100)/3. \quad (1)$$

This equation suggests that, if C_{Te} approaches zero, *M* becomes increasingly large, resulting in a crystal with a long period stacking structure, and that when *M* reaches infinity (the spacing between the diffraction peaks *A* and *B* is zero) at Sb 100%, the structure converges to the *A*7-type Sb.

Rietveld analyses were carried out for the data of the $Sb_{72}Te_{28}$ and $Sb_{85}Te_{15}$ specimens, because of the examined Sb–Te specimens only these two had nearly integral *M* values.[1] The fitting results are shown in Fig. 4. Structural parameters and reliability factors are listed in Tables 1 and 2. For both crystal structures atoms are stacked along the *c* axis, these structures being based on the *ABC* stacking of a cubic close-packed structure. The structure of $Sb_{72}Te_{28}$ is 11*R* ($R\bar{3}m$) and the stacking sequence of close-packed planes is Te–Sb–Te–Sb–Sb–Sb–Sb–Sb–Te–Sb– (repeated three times, because the *ABC* stacking requires that the number of planes within the unit cell is always a multiple of three). The structure of $Sb_{85}Te_{15}$ is 19*R* ($R\bar{3}m$) and the stacking sequence is Te–Sb–Te–Sb–Sb–Sb–Sb–Sb–Sb–Sb–Sb–Sb–Sb–Sb–Sb–Sb–Sb–Sb–Te–Sb– (repeated three times). In these configurations of Sb and Te, we can see that these structures consist of two kinds of structural unit. One is a unit in which Te and Sb are stacked alternately, and the other is a unit in which Sb layers are

[1] Supplementary data for this paper are available from the IUCr electronic archives (Reference: OG5010). Services for accessing these data are described at the back of the journal.

stacked continuously. The former is similar to the NaCl-type atomic configuration, which is characteristic of the Sb_2Te_3 structure, and the latter is similar to the *A*7-type Sb structure. This feature is also seen in the structure of Sb_2Te (Agafonov *et al.*, 1991). The atomic layers are displaced alternately along the *c* axis, showing a kind of modulated structure.

From the results of these structural analyses and the Te-concentration dependence of the stacking period *M*, it is concluded that the crystal structures of the Sb–Te binary system change continuously with Te concentration, as shown in Fig. 5, where the structural units of *A*7-type Sb are shown as yellow solid circles and those of the NaCl-type atomic configuration are blue parallelograms. These two units are located alternately along the direction of the *c* axis. As the Te concentration decreases, the number of pairs of *A*7-type Sb layers that are placed between the NaCl-type units increases. Accordingly, the stacking period increases, shown as a red line in the figure. Although the δ phase is indicated as a eutectic (Sb + Sb_2Te_3) region on the phase diagram (ASM International, 1996), our results show in this phase the existence of a series of successive intermetallic compounds which are formed by intergrowth of these two structural units on the atomic level. Assuming this structural model, we obtained satisfactory Rietveld analyses for the other five Sb–Te specimens.

The chemical formula of each structural model can be expressed as $Sb_{2n}Te_3$ by taking *n* as an integer in Fig. 5. According to this expression, the stacking period *M* is equal to $2n + 3$, and the Te concentration (in at.%) can be represented as $300/M$ by equation (1). The model with $n = 4$ is $M = 2 \times 4 + 3 = 11$, which has an 11*R* structure and a Te concentration of 27.3 at.% and corresponds to the specimen of $Sb_{72}Te_{28}$ in this study. The model with $n = 8$ is $M = 2 \times 8 + 3 = 19$, which has a 19*R* structure and a Te

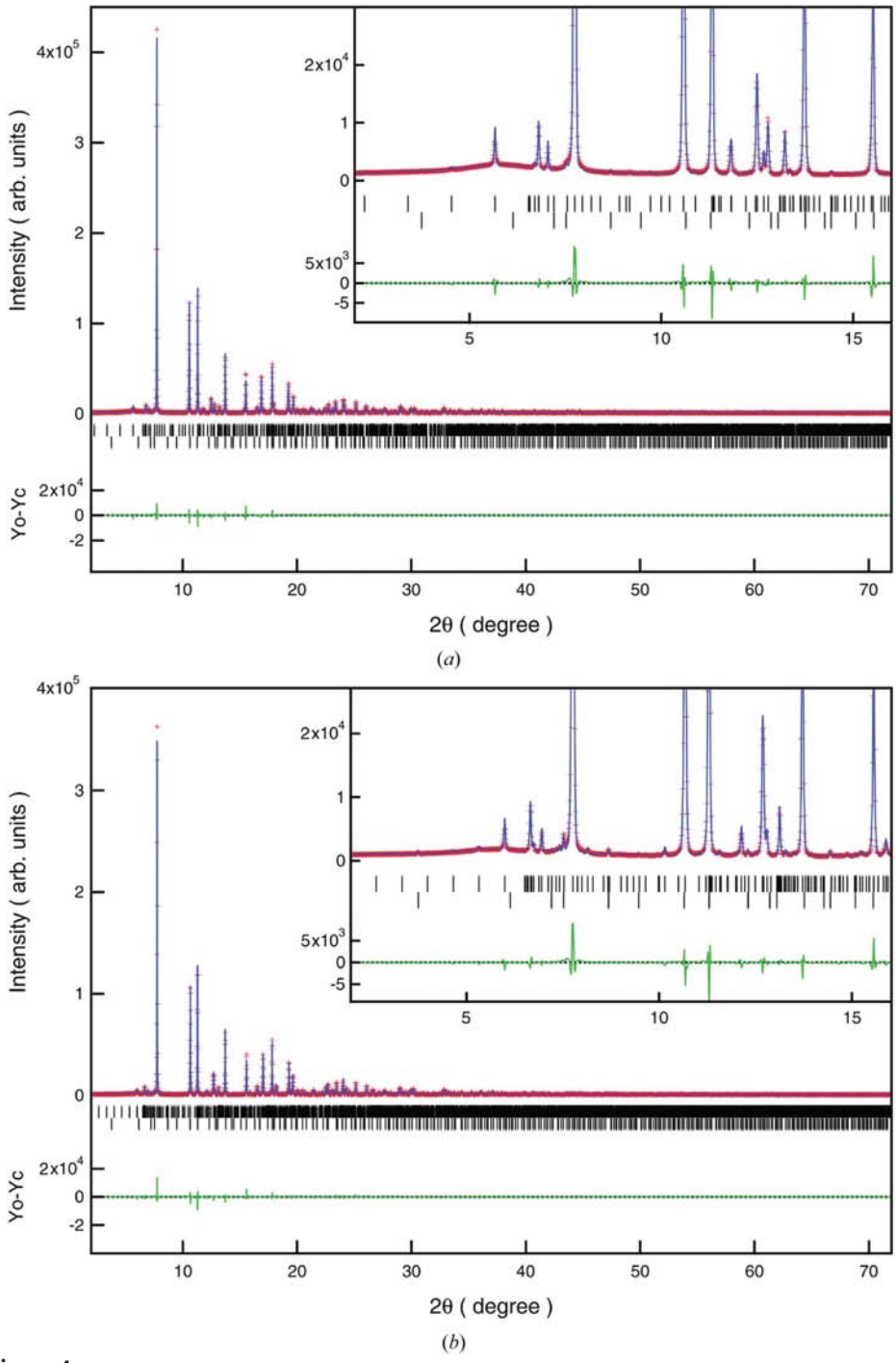

Figure 4
Rietveld fittings for $Sb_{72}Te_{28}$ and $Sb_{85}Te_{15}$. Observed (+) and calculated (blue line) X-ray diffraction profiles of $Sb_{72}Te_{28}$ (top) and $Sb_{85}Te_{15}$ (bottom) at 90 K. The wavelength of incident X-rays is 0.42137 Å. A difference curve (observed–calculated) appears at the bottom of each figure. Weak reflection peaks due to the Sb_2O_3 phase were observed in the profile and a two-phase analysis was carried out. The reflection markers are indicated by vertical bars under the profile (upper: Sb–Te phase; lower: Sb_2O_3 phase).

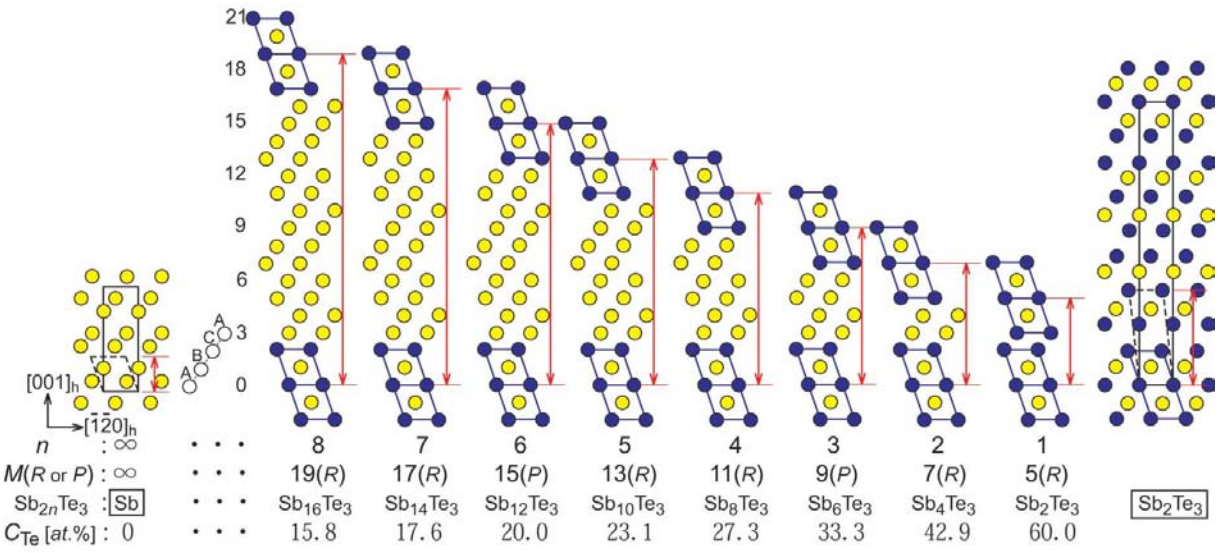

Figure 5
$[100]_h$ projection of crystal structure models of the Sb–Te binary system. Yellow solid circles indicate Sb atoms and blue circles represent Te atoms. In the structures of Sb and Sb_2Te_3, each atom shows a projection of real atomic position and rectangles represent each unit cell. Except for these two structures, each atom shows a projection of ideal atomic position without displacement along the *c* axes. The stacking period *M*, chemical formula and Te concentration are shown under each model.

concentration of 15.8 at.% and corresponds to another specimen of $Sb_{85}Te_{15}$. The following formula is the result

$$M = 2n + 3 = 3 \times 100/C_{Te}. \quad (2)$$

This equation suggests that Te concentration can decrease further; for example, when C_{Te} is 12 at.%, *M* will be 25, the crystal will have a 25*R* structure and the lattice parameter of the *c* axis will increase to 143 Å (= 1.9 × 25 × 3, where the thickness of the fundamental stacking layer is about 1.9 Å). It will be interesting to investigate to what large number the stacking period can be extended; in other words, to confirm the limit of this formula.

As described above, the Sb-rich Sb–Te binary compounds have very complicated structures with a remarkable number of stacking layers in their unit cells, depending on their compositions. However, the phase change materials in practical use (for example, $Ag_{3.4}In_{3.7}Sb_{76.4}Te_{16.5}$ or $Ge_{7.1}Sb_{76.0}Te_{16.9}$) show the *A*7-type structure at room temperature and change to the still simpler structure that can be approximated by a simple cubic structure at higher temperatures (~650–750 K; Matsunaga & Yamada, 2004). On the other hand, we have confirmed in this study that the Sb–Te binary compounds without additional elements such as Ag, In and Ge retain their anisotropic and complicated structures, in which Sb and Te layers are alternately stacked, up to high temperatures. In these compounds, however, it is shown that the crystallization speed becomes faster with the increase of the Sb/Te ratio (Khulbe *et al.*, 2002). As mentioned above, the number of Sb continuous layers with the A7-type atomic configuration increases with Sb concentration. This change of the crystallization speed is presumed to depend on the ratio of these simple A7-type atomic arrangements in the compounds. Khulbe *et al.* have also shown that the stability of the amorphous phase is lost when the Sb/Te ratio is increased. This fact suggests that the Sb and Te mixture is important for the stability of this phase. In addition, these authors found that Ge doping of the Sb–Te binary alloy further stabilizes the amorphous state. As has already been mentioned, this Ge doping contributes simultaneously to simplifying the Sb–Te structure (Matsunaga & Yamada, 2004). Therefore, it is indicated that, in utilization of the phase-change recording materials, added elements such as Ag, In and Ge play very important roles in reconciling two opposing features: the recorded amorphous marks must be stable, but on the other hand, they should be able to be readily and quickly erased. The search for other doping elements that further improve the quality is a subject for future study.

4. Conclusions

The crystal structures of sputtered film specimens were studied in the Sb–Te binary system. Many intermetallic compounds with very long stacking period structures have been discovered. Each structure is based on the cubic close-packed structure and the stacking period changes continuously, according to a simple law, with composition. If Te concentration is adjusted, a structure with an extremely long stacking period can be formed.

The synchrotron radiation experiments were performed at SPring-8 with the support of the Japan Synchrotron Radiation Research Institute (JASRI) (Proposal No. 2004-A0492-ND1c-np), and the authors express sincere thanks to Dr K. Kato and Dr M. Takata for their kind help for the diffraction measurements.

References

Agafonov, V., Rodier, N., Ceolin, R., Bellissent, R., Bergman, C. & Gaspard, J. P. (1991). *Acta Cryst.* C**47**, 1141–1143.

ASM International (1996). *Binary Alloy Phase Diagrams*, 2nd ed., plus updated Version 1.0 on CD-ROM, edited by T. B. Massalski, H. Okamoto, P. R. Subramanian & L. Kacprzak. Materials Park, Ohio: ASM International.

Clark, G. L. (1955). *Applied X-rays.* New York: McGraw-Hill.

Iwasaki, H., Ide, Y., Harigaya, M., Kageyama, Y. & Fujimura, I. (1992). *Jpn. J. Appl. Phys.* **31**, 461–465.

Khulbe, P. K., Hurst, T., Horie, M. & Mansuripur, M. (2002). *Appl. Opt.* **41**, 6220–6229.

Matsunaga, T., Umetani, Y. & Yamada, N. (2001). *Phys. Rev. B*, **64**, 184116.

Matsunaga, T. & Yamada, N. (2004). *Jpn. J. Appl. Phys.* **43**, 4704–4712.

Nakata, Y., Suenaga, T., Ejiri, M., Shida, S., Tani, K., Yiwata, N. & Tashiro, H. (2004). *Mater. Trans.* **45**, 2673–2677.

Takata, M., Nishibori, E., Kato, K., Kubota, Y., Kuroiwa, Y. & Sakata, M. (2002). *Adv. X-ray Anal.* **45**, 377–384.

Wyckoff, R. W. G. (1963). *Crystal Structures*, 2nd ed. New York: Interscience.

Yamada, N., Ohno, E., Nishiuchi, K., Akahira, N. & Takao, M. (1991). *J. Appl. Phys.* **69**, 2849–2856.